Dynamics of liquid Au from neutron Brillouin scattering and *ab initio* simulations: Analogies in the behavior of metallic and insulating liquids

E. Guarini,[1] U. Bafile,[2] F. Barocchi,[1] A. De Francesco,[3] E. Farhi,[4] F. Formisano,[3] A. Laloni,[3] A. Orecchini,[4,5] A. Polidori,[5] M. Puglini,[1] and F. Sacchetti[5]

[1]*Dipartimento di Fisica e Astronomia, Università di Firenze, via G. Sansone 1, I-50019 Sesto Fiorentino, Italy*
[2]*Consiglio Nazionale delle Ricerche, Istituto dei Sistemi Complessi, via Madonna del Piano 10, I-50019 Sesto Fiorentino, Italy*
[3]*Consiglio Nazionale delle Ricerche, Istituto Officina dei Materiali, Operative Group in Grenoble (OGG), c/o Institut Laue Langevin, 6 rue Jules Horowitz, BP 156 F-38042 Grenoble Cedex, France*
[4]*Institut Laue Langevin, 6 rue Jules Horowitz, BP 156 F-38042 Grenoble Cedex, France*
[5]*Dipartimento di Fisica, Università di Perugia, via A. Pascoli, I-06123 Perugia, Italy*

(Received 18 June 2013; revised manuscript received 18 August 2013; published 20 September 2013)

We performed a neutron Brillouin scattering determination of the dynamic structure factor of liquid gold in the wave-vector range $6 < Q < 16$ nm^{-1}. Despite the experimental difficulties due to the considerable neutron absorption and the high melting temperature of the sample, a non-negligible coherent signal could successfully be extracted and revealed the presence of underdamped ion density-fluctuation modes in the whole Q range of the experiment. The quality of the data further enabled a significant comparison with the results of *ab initio* simulations for liquid gold. The agreement found between neutron and simulation data not only provides a necessary test of *ab initio* methods still limited to the use of few hundreds atoms, but also reasonably justifies a thorough analysis of the simulated dynamics in the extended Q range that can be more comfortably accessed by calculations. A viscoelastic modeling of the simulated spectra proves to be appropriate and, surprisingly, the so-derived salient dynamic features of liquid gold show an overall Q behavior globally similar to that already found for insulating liquids. The present and recent results on the collective properties of simple liquids thus lead us to embrace the concept that simple liquid metals and insulators, at the nanometer length scale, are dynamically much less different than expected.

DOI: 10.1103/PhysRevB.88.104201 PACS number(s): 61.25.Mv, 61.05.fg, 61.20.Ja

I. INTRODUCTION

Since the first neutron measurements on lead and rubidium by Copley and coworkers,[1,2] the dynamics of liquid metals has been a major topic of the physics of the liquid state for several reasons. First of all because pure metals are, along with rare gases, the paradigm of simple fluids, for which the purely translational nature of the atomic (ionic) motions largely simplifies the modeling and description of spectroscopic data. Another reason for the great interest in liquid metals is the typically high visibility[3] of inelastic peaks related to longitudinal acoustic modes in the dynamic structure factor $S(Q,\omega)$ obtained by neutron or x-ray scattering. Such a visibility is of course always helpful in detecting the dynamics of the collective excitations in any system. However, in the 1980s, scientists in the field of liquid dynamics attributed a special significance to studies of liquid metals because of the misleading conviction that collective modes could be proved to exist only if directly visible as real (relative) maxima in the dynamic structure factor.[4] With such a belief, liquid metals guaranteed, more than other fluids, the possibility to follow the dynamics of excitations up to rather high Q values and to assess the validity of available models for $S(Q,\omega)$ also with decreasing the explored length scale. It is worth recalling that inelastic peaks are enhanced in the spectra of liquid metals because the specific-heat ratio γ is often close to unity and, at the same time, the sound velocity is higher than in other rare-gas or molecular liquids. These facts together generally deplete the central line in favor of well-separated inelastic lines. However, not all liquid metals have γ close to unity.[5] Moreover, a good visibility is not so peculiar of liquid metals.[6] Furthermore, it is presently widely accepted that apparently featureless spectra often contain inelastic contributions, and that excitation modes actually survive at much larger Q values than those suggested by a naked-eye observation of the spectral shape.[7]

Nonetheless, spectroscopic studies (by x-ray or neutron inelastic scattering) of several molten pure metals (Pb,[2,8,9] the alkali metals,[1,10,11] Hg,[12–14] Ga,[15] Ni,[16,17] Zn,[18] Cd,[19] Al,[20] Bi,[8,21] Sn,[22] Fe,[23] Mg,[24] and Ti[25]) as well as of semimetals,[26] binary alloys,[27–29] and metal solutions[30–33] greatly contributed to the present knowledge about the dynamic response of a fluid at equilibrium. The objectives of such measurements and, sometimes, of corresponding simulations, were increasingly refined: from the determination of the damping and dispersion of ionic acoustic modes, to the test of different models for the dynamic structure factor, to the indirect study of the electron-gas properties, and finally to the determination of effective ion-ion interaction potentials. It is worth anticipating that, as regards the dynamic properties of gold, we first focused on the first two aspects mentioned above, which are also tackled in detail in a recent book about the state of the art in liquids dynamics.[3] There, a strong effort is done to clarify whether acoustic excitations in liquids have a somewhat universal behavior or not, independently of the metallic or insulating nature of the system. With a similar spirit, and taking advantage of some experience of ours in molecular liquids dynamics,[6,34–36] we addressed the study of a few unexplored metals,[18,19] and of gold in particular.

Concerning the comparison between liquid metals and insulators from the dynamic point of view, scientists in the field are now left with a few but very general open questions. The first is why at the length scales probed by neutrons or x-rays, the quasielastic and inelastic spectral line widths are of the same order of magnitude for liquids of both classes and do not reflect at all the much larger thermal conductivity of metals, which is very much enhanced by the electronic contribution, absent in insulating fluids. The second regards the dynamic behavior of metals as Q is decreased: on the one hand, the sound velocity seems generally to reach the hydrodynamic values at the lowest wave vectors accessed by neutrons or x-rays ($\simeq$1 nm^{-1}); on the other hand, the sound damping really does not. For instance, the dynamics of liquid nickel measured by x-rays[16] provides a clear, but not at all unique, example of this typical behavior in molten metals. The situation is even clearer when the damping of the thermal mode is analyzed, finding that low-Q experimental data dramatically deviate from the huge values that would be expected on the basis of the hydrodynamic Q^2 behavior. Indeed, the true difference between metallic and insulating liquids seems to be the Q range where complete hydrodynamic behavior is reached:[3] apparently, for liquid metals, this happens at much larger length scales than in insulating liquids.[6,16,36]

The reasons for an experimental investigation of the microscopic dynamics of liquid gold deserve the next, specific, section of this work. The remainder of the paper will then describe experimental details and data analysis procedures (Sec. III), the comparison of the experimental results with *ab initio* simulations performed by the Computing for Science group of the Institut Laue-Langevin (ILL) in Grenoble (Sec. IV), and the presentation of liquid gold dynamical parameters in comparison with those obtained for completely different (insulating) systems (Sec. V). Conclusions are drawn in Sec. VI.

II. INTEREST IN COLLECTIVE DYNAMICS OF GOLD AND SUITABLE TECHNIQUE

Like all pure liquid metals, gold is a simple monatomic fluid, but no spectroscopic measurement was devoted so far to explore its dynamic behavior, about which only a very recent *ab initio* simulation work is reported in the literature.[37] Certainly, difficulties such as the considerable absorption and high melting temperature of gold (1337 K) have long discouraged experimentalists: the former being more critical in inelastic scattering measurements, where an acceptable statistics must be achieved at each energy channel of the experimental spectra. Differently, diffraction measurements on liquid gold were carried out by Waseda and Ohtani in the mid 1970s[38] in order to derive its static structure factor $S(Q)$.

With the aims previously mentioned, an important fact is that in liquid gold γ differs appreciably from unity ($\gamma = 1.5$) and is, for instance, fully comparable with that of an insulating liquid such as methane ($\gamma = 1.6$). The heat mode of the spectrum has then enough intensity to allow for the observation of a high thermal conductivity.

Another interesting property is that, among the other elements of the periodic table, gold presents (together with mercury) the strongest *relativistic effects*,[39] one of which is due to the high velocity of electrons in high-Z elements, since $v_e \simeq \frac{Z}{137}c$. For gold $Z = 79$, thus $v_e \simeq 0.58c$, so that the relativistic mass differs appreciably from that at rest (23% in gold), with a consequent shrinking of the s and p orbitals. This, combined with other spin-orbit coupling effects, eventually results in a reduction of the gap between the $6s$ and $5d$ orbitals of gold giving rise to particular properties that would be otherwise absent, the most spectacular one being the color of gold itself, since it absorbs blue light. As it was suggested for mercury, relativistic effects influence the interaction potential;[40] thus the ionic dynamics might significantly be modified as well. For instance, the reduction of the dispersion attraction in the interatomic potential of mercury, observed by using relativistic and nonrelativistic all-electron methods to study the binding energy of Hg,[41] was found to originate from relativistic effects. Consequently, quantities like the dynamic structure factor might prove very useful to reveal their presence, given the undoubtful sensitivity of $S(Q,\omega)$ to the shape of the interaction potential.[34] The role of relativistic effects on the interaction properties and on the resulting microscopic dynamics certainly warrants further investigations in liquid metals and, first of all, of spectroscopic measurements on liquid gold.

Another important aspect that encouraged measurements on gold and other metals was the availability of *ab initio* simulations, to which the Computing for Science Group of the ILL devoted a strong effort in recent years. The computational activity deserved a comparable experimental effort, aimed at verifying the reliability of calculations which, at present, can be performed with a number of particles limited to a few hundred, to be compared with the thousands of classical molecular dynamics (MD).

In this work, however, postponing the study of effective potentials through a joint use of experiments and extended MD, we focus on the investigation of the collective excitations of liquid gold and the comparison of some of their properties with those of other fluids, both metallic and insulating.

From the experimental side, one needs to consider that gold very willingly absorbs both neutrons and x-rays. For x-rays the situation is critical for high-Z elements, since photoelectric absorption grows as Z^4 and the corresponding intensity loss is not compensated by the Z^2 growth of the scattering cross section. Neutron absorption by gold is conspicuous too, with respect to other nuclei, but the absorption and scattering cross sections are such ($\sigma_{abs} = 54.2$ b at 1 Å incident wavelength, $\sigma_s = 7.75$ b) that the absorption-to-scattering ratio is even slightly smaller than for other highly absorbing samples, such as mercury and special mixtures of cadmium isotopes, that were very successfully investigated by inelastic neutron scattering.[12,19] Neutrons are also eligible because of the advantageous shape of the instrumental energy-resolution function.

The most significant Q region in studies of the collective dynamics of liquids typically extends from a few inverse nanometers (where departures from hydrodynamic behavior start to show up also in the dispersion curve of insulating liquids) to values close to the position Q_p of the main maximum in the static structure factor ($Q_p = 26$ nm^{-1}, for gold). In neutron spectroscopy such a region is often named the neutron Brillouin scattering (NBS) one. In presence of systems with a rather high sound velocity ($c_s = 2568$ m/s

in gold[5]), an adequately high incident energy is required to properly probe the excitation modes, thus the (low) Q values typical of NBS can be spanned only by means of small-angle detection. The time-of-flight (TOF) spectrometer BRISP at the ILL was designed exactly with this purpose by exploiting thermal neutrons and a detection area around the direct beam.[42] BRISP was thus employed for the experimental investigation of the dynamics of gold in the range $6 < Q < 16$ nm^{-1}. Note that the use of a TOF instrument is very convenient when dealing with strongly absorbing samples, so to achieve an acceptable statistical accuracy with nonprohibitive beam-time needs, through the simultaneous collection of all neutrons scattered in the whole angular range of the instrument detector.

III. EXPERIMENTAL DETAILS AND EXTRACTION OF $S(Q,\omega)$

The sample (28 g of Au chunks) was liquefied directly inside a molybdenum slab container (inner volume $w \times h \times t = 26 \times 40 \times 1.8$ mm^3, with two 1-mm-thick walls in the beam direction) placed inside a furnace maintained at 1373 K, i.e., just above the melting point of gold and well below the melting temperature of molybdenum (2890 K).[43] The scattering, absorption, and geometrical properties of the sample corresponded to a 55% transmission at the number density of liquid gold ($n = 53$ nm^{-3}).[5] A boron nitride mask on the entrance wall of the cell was used to reduce the scattering from the container and to properly adjust the illuminated area ($w \times h = 26 \times 33$ mm^2) according to the height (about 35 mm) reached by the liquid in the cell.

The highest incident energy available on the BRISP spectrometer ($E_0 = 83.8$ meV, $\lambda_0 = 0.988$ Å) was selected by exploiting the pyrolytic-graphite (004) reflection of the instrument monochromator. The detector was placed 4 m from the sample position in order to reach scattering angles below 15°.

In addition to the sample runs, the usual background and empty-cell measurements were performed. The energy resolution of the instrument in the chosen setup was determined by collecting the intensity scattered by a vanadium foil (1 mm thickness) inserted in the empty cell. After proper consideration of the various effects affecting the vanadium raw data (e.g., background, multiple scattering, and self-attenuation), the corrected vanadium spectra turned out to have the Gaussian shape typical of the elastic resolution function of neutron spectrometers. In particular, the Gaussian fits to the vanadium spectra yielded a full width at half maximum (FWHM) of 3.1 meV. Also, the vanadium integrated intensities provided the required link between experimental and absolute units, thanks to the knowledge of the mainly elastic and incoherent neutron scattering law of such a reference sample. Negligible dependence on Q was observed for both the vanadium spectral widths and integrated intensities. An example of a vanadium spectrum, along with its Gaussian fit curve, is reported in Fig. 1 for $Q = 6$ nm^{-1}.

Here and in the following Fig. 2, the experimental spectra are displayed as a function of the exchanged energy $E = \hbar\omega$ in units of meV just to allow an immediate understanding of the experimental ranges and related instrument setup by neutron experimentalists. In the remainder of this paper the angular

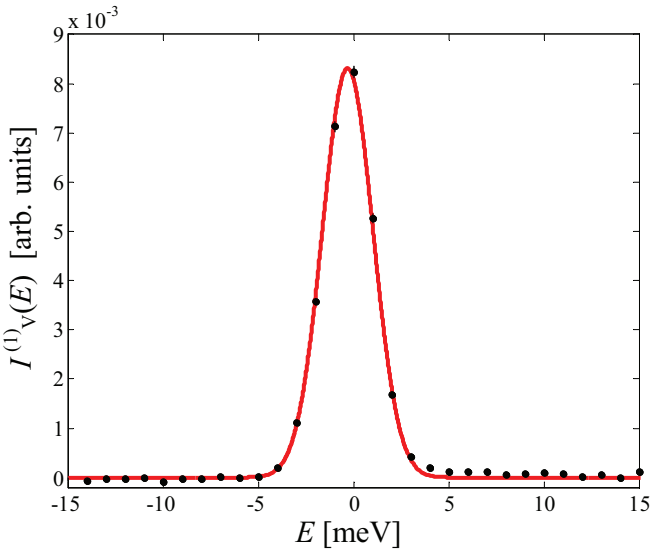

FIG. 1. (Color online) Single-scattering intensity of the vanadium sample at $Q = 6$ nm^{-1} (dots with error bars) and Gaussian fit curve (red line).

frequency ω in units of ps^{-1} will be preferred as spectral variable to facilitate comparisons with other published data.

When studying the collective properties, we enter the realm of the so-called "coherent" neutron scattering, since the sought-for quantity, i.e., the total dynamic structure factor $S(Q,\omega)$, is weighted by the coherent cross section $\sigma_{\rm coh} = 4\pi b^2_{\rm coh}$ in the general expression of the neutron double-differential cross section:

$$\frac{d^2\sigma}{d\Omega d\omega} = \frac{k_1}{k_0}\tilde{S}(Q,\omega) = \frac{k_1}{k_0}\left[b^2_{\rm coh}S(Q,\omega) + b^2_{\rm inc}S_s(Q,\omega)\right]. \quad (1)$$

In Eq. (1), where k_1 and k_0 are the scattered and incident neutron wave vectors, respectively, and the bs are the scattering lengths of the Au atomic species, the neutron combination $\tilde{S}(Q,\omega)$ of the total and self- (subscript s) dynamic structure factors is explicitly indicated. In the presence of a nonzero incoherent cross section $\sigma_{\rm inc} = 4\pi b^2_{\rm inc}$, one needs to get rid of the last term. The cross-section values of gold ($\sigma_{\rm coh} = 7.32$ b and $\sigma_{\rm inc} = 0.43$ b) might erroneously suggest a negligible incoherent contribution for this system. On the contrary, incoherent scattering largely influences the neutron intensities whenever the coherent component, proportional to $S(Q)$, is probed at the rather small Q values of NBS, where the static structure factor does not depart appreciably from $S(0)$ which, for dense liquids, is typically rather small (0.0132 for gold at the melting point) due to the very low compressibility of the liquid. Thus, account must be taken of the contribution of $S_s(Q,\omega)$. In our conditions this is quite an easy task, because experimental intensities depend on the resolution-broadened version of Eq. (1), so that spectral components much narrower than the instrument resolution actually reduce, upon broadening, to a Gaussian shape proportional to the normalized resolution function $G_0(\omega)$ of the neutron spectrometer. This is exactly the case with the present measurements on gold. Indeed, the FWHM of the self-, diffusive-like, spectrum is given in the hydrodynamic regime by $2DQ^2$, with $D = 3.5 \times 10^{-9}$ m^2/s.[44] However,

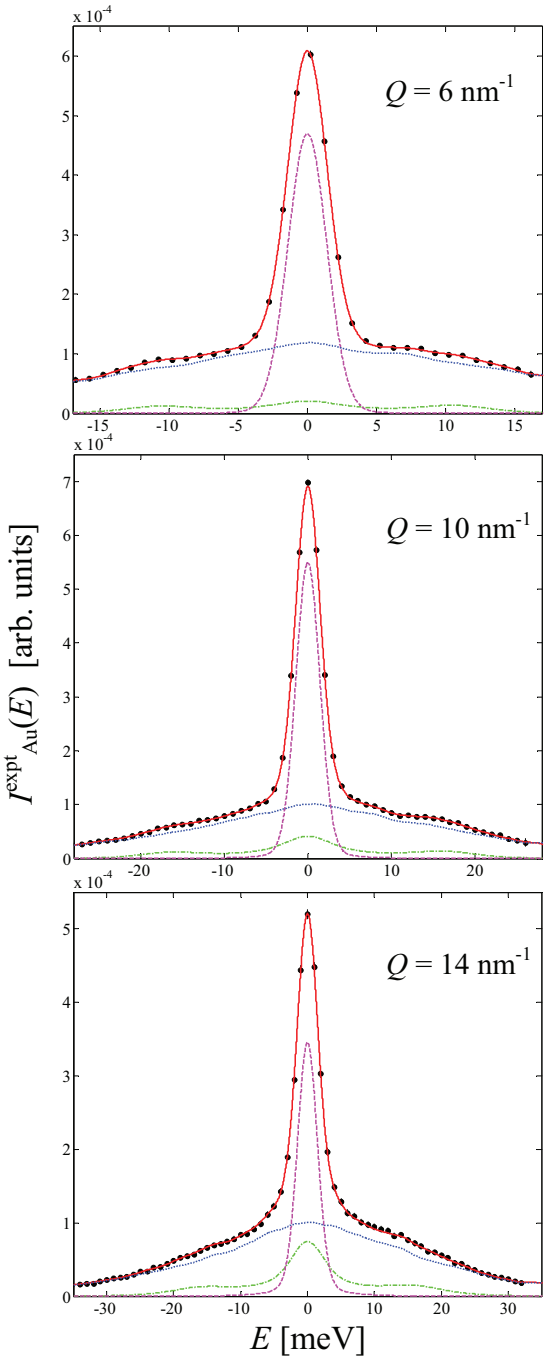

FIG. 2. (Color online) Neutron data (dots with error bars) at three experimental Q values compared with the global fit curve (solid, red) obtained with the modeling summarized in Eqs. (3) and (4). The various components of Eq. (3), i.e., the coherent (green dash dots), incoherent (magenta dashes) and double scattering (blue dots) signals, are also shown.

with increasing Q in the range of this experiment, it is well known that in any liquid the width displays a progressively weaker Q dependence, so that one can take the hydrodynamic Q^2 behavior as an upper bound to the FWHM of $S_s(Q,\omega)$. Doing so, we find that, even at our highest Q value, the self-spectrum is narrow enough to be well represented by $S_s(Q,\omega) \approx \delta(\omega)$. The incoherent part of the measured signal can thus be confidently modeled as proportional to $b_{\rm inc}^2 G_0(\omega)$ when BRISP resolution effects are taken into account.

Inelastic neutron scattering measurements do not directly provide the double-differential cross section, but a counting rate per unit frequency that can be schematized as

$$I^{\rm expt}(Q,\omega) = C\left[\frac{d^2\sigma}{d\Omega d\omega}\right]_{\rm asym,b} + I^{(m)}(Q,\omega). \qquad (2)$$

Here, $d^2\sigma/(d\Omega d\omega)$ refers to the sample scattering only and is obtained by subtracting the background and the empty-cell signal properly attenuated by sample absorption, and by accounting for the weakly-energy-dependent part of detector efficiency and self-shielding. The double-differential cross section is at this point still affected by detailed-balance asymmetry and the energy resolution broadening, synthetically recalled by the subscripts asym and b. The instrumental normalization factor C, here including also the average sample-plus-cell attenuation factor, can be estimated as being proportional to the amplitude of the Gaussian fits of the vanadium spectra if, as it was in our case, the vanadium and sample geometries strongly resemble each other. The experimental intensity would thus directly provide, combining Eqs. (1) and (2), the sought-for $\tilde{S}(Q,\omega)$, if the multiple scattering (unwanted) component $I^{(m)}(Q,\omega)$ were absent. Unfortunately, multiple scattering is never negligible in inelastic-scattering measurements, not even in the presence of samples with a limited scattering power, as it was in our case (7%). Due to the typically narrow energy region where single scattering is important and, conversely, to the broad energy distribution of the multiple-scattering intensity, the latter contribution is large in the tails and fully dominant in the far wings of the spectra. Therefore, a reasonable data analysis should at least contemplate the evaluation of double scattering, since it retains a weak but well-defined energy dependence, while higher-order components can usually be approximated by an additional flat background. To obtain the energy dependence of the double-scattering intensity we recently developed a very efficient code based on multidimensional Monte Carlo integration of appropriate functions detailed in Ref. 45. Finally, the calculated quantities were employed in a global fit to the experimental spectra of a model function, based on the quoted approximations, namely:

$$I^{\rm fit}(Q,\omega) = C\frac{k_1}{k_0}\left\{\left[b_{\rm coh}^2 S_{\rm GH}(Q,\omega)\right]_{\rm asym,b} + b_{\rm inc}^2 G_0(\omega)\right\} + K_m I^{(2)}_{\rm calc}(Q,\omega), \qquad (3)$$

where K_m and C are two of the six free parameters of the fit; the former providing the necessary factor to convert the calculated double-scattering energy distribution $I^{(2)}_{\rm calc}(Q,\omega)$ into an intensity profile consistent with the arbitrary units of the experimental data. Here the subscripts asym and b indicate that, within the fit algorithm, the model lineshape is given the correct asymmetry and is broadened by an explicitly performed convolution with $G_0(\omega)$. On the other hand, $I^{(2)}_{\rm calc}(Q,\omega)$ does not require to be similarly broadened, being by itself broad enough to remain unaffected by the convolution. As far as C is concerned, a good agreement was found between the fit result and the expected value obtained

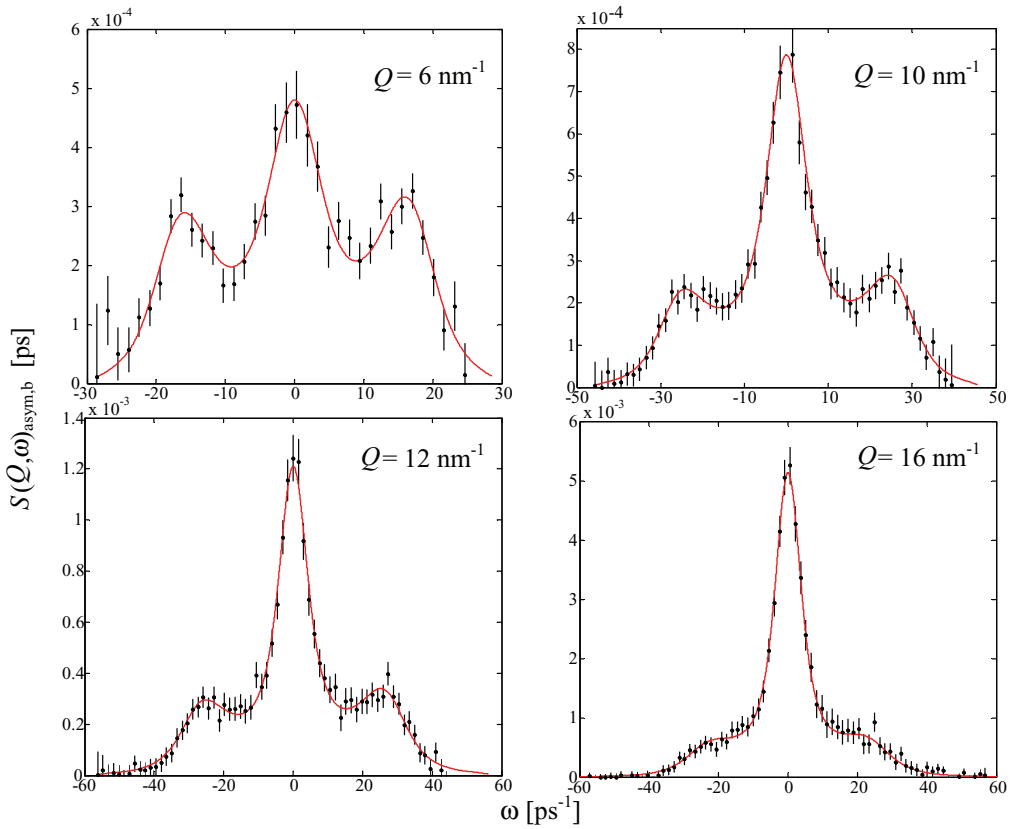

FIG. 3. (Color online) Dynamic structure factor of gold at four Q values of the NBS experiment. The experimental data (black dots with error bars) are broadened by the instrumental energy resolution. The corresponding fit by means of the GH model (red solid line) has been carried out taking detailed-balance asymmetry and resolution into account. The curve fit is the same as the green line in Fig. 2, although in different units.

from the vanadium measurements and from knowledge of the sample-container geometry and transmission. The other free parameters of the fit are contained in the generalized hydrodynamics (GH) modeling of the dynamic structure factor which, in its symmetric (i.e., "classical") form, is given by[46]

$$S_{\mathrm{GH}}(Q,\omega) = \frac{S(Q)}{\pi}\left[a_0\frac{z_0}{z_0^2+\omega^2} + a_{\mathrm{s}}\frac{z_{\mathrm{s}}+b_{\mathrm{s}}(\omega+\omega_{\mathrm{s}})}{z_{\mathrm{s}}^2+(\omega+\omega_{\mathrm{s}})^2} + a_{\mathrm{s}}\frac{z_{\mathrm{s}}-b_{\mathrm{s}}(\omega-\omega_{\mathrm{s}})}{z_{\mathrm{s}}^2+(\omega-\omega_{\mathrm{s}})^2}\right], \tag{4}$$

where the Q dependence of the fit parameters a_0, z_0, z_{s}, and ω_{s} was omitted to shorten the notation. Combinations of the amplitude and half width of the central Lorentzian line (subscript 0) representing the thermal nonpropagating mode, together with the damping z_{s} and frequency ω_{s} of the sound modes can be shown[46] to determine the amplitude a_{s} and asymmetry factor b_{s} of the inelastic lines. Moreover, the reduced second frequency moment $\langle\omega_Q^2\rangle$, i.e., the second moment of the normalized spectrum $S(Q,\omega)/S(Q)$, is obtained in the GH modeling as

$$\langle\omega_Q^2\rangle = z_{\mathrm{s}}^2+\omega_{\mathrm{s}}^2 - a_0[(z_0-z_{\mathrm{s}})^2+\omega_{\mathrm{s}})^2] \tag{5}$$

[see Eqs. (49a) and (49c) of Ref. 46]. By comparison with the theoretical value $\langle\omega_Q^2\rangle = k_{\mathrm{B}}TQ^2/[mS(Q)]$ an evaluation of $S(Q)$ is obtained as a function of the free fit parameters. In the above formula, k_{B} is the Boltzmann constant, T is the temperature, and m is the atomic mass.

More refined models for the dynamic structure factor could not be employed in the fit to the experimental data, owing to the growing number of free parameters to be determined in presence also of the quoted unwanted contributions to the measured intensity. Nonetheless, a GH modeling of the interesting part of the signal provided more than satisfactory results, of good reliability for comparisons with the simulation outputs, as well as an experimental determination of the dispersion curve and other basic parameters characterizing the collective dynamics of liquid gold. An example of the quality of the fit of Eq. (3) to the sample spectra is given in Fig. 2, where the coherent, incoherent, and double-scattering contributions are also separately displayed at three Q values.

By subtracting the fit-derived incoherent and multiple-scattering components from $I^{\mathrm{expt}}(Q,\omega)$, one obtains, after normalization to absolute units, an experimental determination of the dynamic structure factor $S(Q,\omega)_{\mathrm{asym,b}}$, shown in Fig. 3 at selected Q values. The displayed uncertainties are rather large due to the error propagation from the raw data statistics through the subtraction of all the other contributions to the total signal. In Fig. 3 we also plot the GH description, as obtained from the same fit performed with the model function in Eq. (3). The corresponding Q dependencies of some of the GH fit parameters are reported in Fig. 4. In particular, the frequency and damping rate of the collective sound

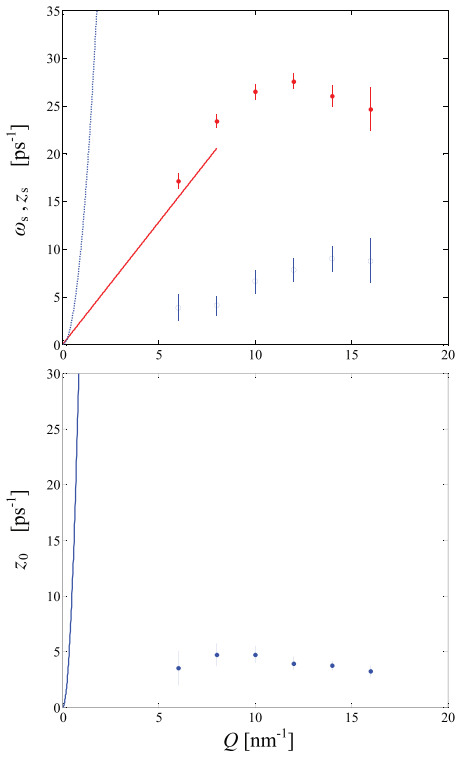

FIG. 4. (Color online) Top panel: frequency (red dots with error bars) and damping (blue circles with error bars) of the acoustic modes of gold as a function of Q, as obtained from the GH fits of the experimental data. The hydrodynamic behaviors are also shown for both quantities: a solid red line for the frequency and a dotted blue parabola for the damping. Bottom panel: Q dependence of the thermal damping GH parameter (symbols with error bars) compared with the corresponding hydrodynamic prescription (solid parabola).

modes (top frame), as well as the half width of the central thermal mode (bottom frame), are compared with the exact $Q \to 0$ asymptotic prescriptions of the hydrodynamic theory; namely, $c_s Q$, ΓQ^2, and $D_T Q^2$, for ω_s, z_s, and z_0, respectively, calculated for gold by using the quoted value of the adiabatic sound velocity, a sound damping coefficient $\Gamma = 1.1 \times 10^{-5}$ m^2/s,[5,47,48] and a thermal diffusion coefficient $D_T = 4.3 \times 10^{-5}$ m^2/s.[47,49] These quantities have been obtained from the known electrical properties of Au through the use of the Wiedemann-Franz law,[47] where the small ionic contribution is neglected. Inspection of Fig. 4 readily shows that gold dynamically behaves as other conducting liquids at the present length scales,[3] where huge deviations of the sound and thermal dampings from the hydrodynamic parabolic trends are indeed observed.

As for other metals, gold too witnesses the impossibility to probe the true hydrodynamic behavior of the damping of the modes, at the Q values accessible by x-ray or neutron spectroscopy.[3] It has been suggested that damping rates in liquid metals are comparable with those of ordinary liquids because, at the length scales of the quoted spectroscopic techniques, the electronic and ionic dynamics are decoupled to such an extent that these probes only reveal the damping associated with the ions.[3] Differently, the frequencies of the acoustic excitations appear to tend to the hydrodynamic line even at Q values greater than those typical of NBS minimum wave-vector ranges. This suggests that the velocity of sound is little sensitive to the electronic properties. Finally, from the dispersion curve of Fig. 4 it can be observed that, owing to the ordinary-liquid-like values of the experimental sound damping, underdamped acoustic modes propagate in liquid gold up to the maximum Q of the experiment.

The spectra in Fig. 3 are characterized by very-well visible inelastic peaks, which would appear even more prominent if the resolution broadening were corrected for. This confirms that gold behaves in this respect as most other metals, but, at the same time, also provides a convincing proof that such evident excitations can be effectively revealed and investigated even in cases where, as shown in Fig. 2, the raw spectra would, at first sight, suggest quite a different situation.

IV. COMPARISON WITH *AB INITIO* SIMULATIONS

As mentioned in the introduction, among the motivations of the present measurements on liquid gold there was also the important opportunity to verify the effectiveness of *ab initio* simulation methods in reproducing the real dynamic behavior of molten metals. Gold was one of the many conducting liquids that the Computing for Science group of ILL simulated in recent years by means of the Vienna Ab Initio Simulation Package (VASP).[50] VASP is a density functional theory (DFT) code[51] using the generalized gradient approximation (GGA).[52] The projector-augmented wave potentials (PAW)[53] with the Perdew-Burke-Ernzerhof (PBE) exchange correlation functional[54] have been employed to describe electronic states. For gold (d element), the potential energy cutoff is 230 eV. The software in version 5.2.8 has been used in its molecular dynamics mode, which determines iteratively the atom positions.

The liquid gold molecular dynamics simulation has been performed using 200 atoms in a 1.557-nm-edge-length cube, corresponding to a density $\rho = 17.3$ g/cm^3. This configuration sets the smallest excitation wave vector at $Q = 2\pi/1.557 = 4.1$ nm^{-1}, and the intrinsic energy spacing at 0.05 meV. The molecular dynamics simulation was first equilibrated in the NVT canonical ensemble around $T = 1350$ K, for 9 ps (3000 steps of 3 fs). The thermalized atom distribution was then simulated in the NVE microcanonical ensemble for a duration up to 36 ps, in 12 000 time steps of 3 fs. The temperature during the trajectory remained in the range $T = 1387 \pm 78$ K, slightly above the melting point.

The dynamic structure factor was obtained from the trajectories by space and time Fourier transforms, using the nMOLDYN/MMTK software.[55] The momentum and energy smoothing filters used in the fast correlation algorithm were set to 0.5 nm^{-1} and 1 meV respectively. These quantities define an effective resolution assigned to the dynamic structure factor.

The good agreement between the simulation results and experiment can be appreciated, at three example wave vectors, in Fig. 5, where the comparison is performed between the asymmetrized, energy-broadened, simulated spectra and the GH fit curves already shown in Fig. 3.

Such an agreement has been found at all the experimental Q values and constitutes an important confirmation about the quality and reliability of the present *ab initio* calculations.

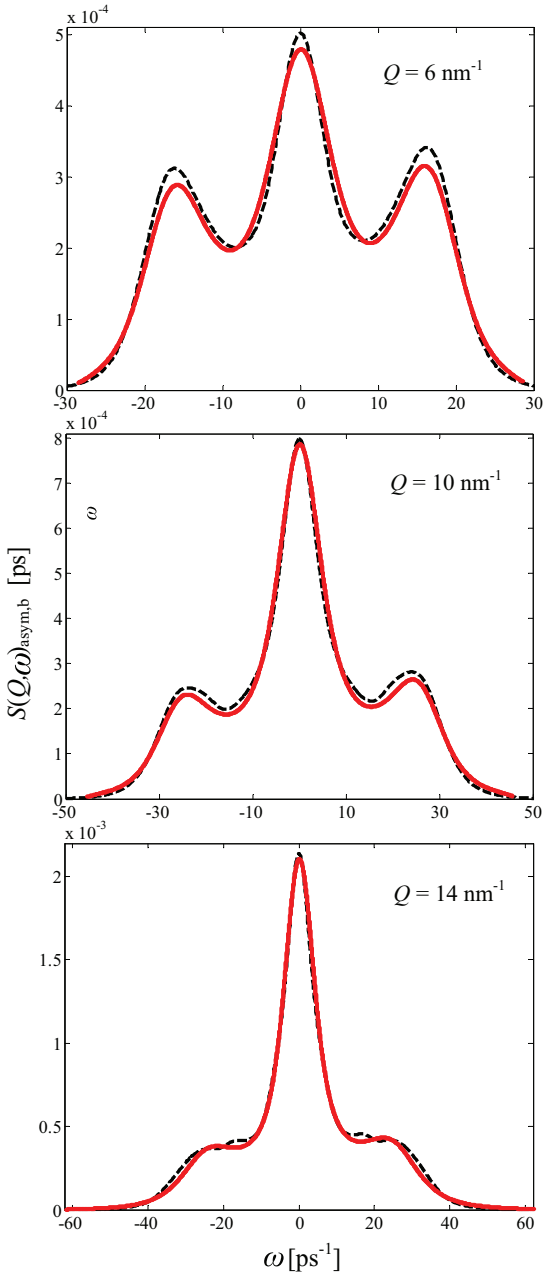

FIG. 5. (Color online) Comparison between the dynamic structure factor of gold as obtained by means of *ab initio* simulations (black dashes) and by the GH modeling of the experimental data (red solid line) already reported in Fig. 3. The simulation spectra have been asymmetrized and convoluted with the experimental resolution function.

Although the comparison could be carried out at the limited number of experimental wave vectors, the encouraging results induced us to exploit the simulation outputs to extend the study of the dynamic properties of gold to a wider kinematic range. The analysis of the simulations is described in the next section.

The just-remarked similarity of the broadened simulated $S(Q,\omega)$ to the one obtained from the GH fit of Eqs. (3) and (4) to the neutron data does not exempt us from noting a slight difference in shape at frequencies around the inelastic peak position, as it appears in Fig. 5. We will postpone to the next section a comment on this point.

V. ANALYSIS OF SIMULATED SPECTRA AND DISCUSSION

We now concentrate on the analysis of the collective dynamical properties of gold as obtained by means of a viscoelastic (VE) modeling (see, e.g., Refs. 46 and 56) of the simulated dynamic structure factor. As observed for most liquids, a viscoelastic description turns out to be slightly superior to the generalized hydrodynamics description, although it requires the determination of a higher number of free parameters. In fact, both the GH and VE models can be shown to descend, in the language of memory functions for the time evolution of the correlation function $F(Q,t)$,[56] from second-order memory functions $M^{(2)}(Q,t)$ of identical structure, i.e., as a linear combination of "viscous" and "thermal" time decays, but with the difference that in the GH case the viscous decay is assumed to be extremely fast with respect to the time scale involved in relaxation processes of thermal origin. A straightforward consequence of such a difference is that the GH spectrum is simpler (a triplet) than the VE one (four-line spectrum).

The time evolution of the intermediate scattering function $F(Q,t)$ of a classical fluid can be described as dependent on the second-order memory function via a generalized Langevin equation of the kind

$$\ddot{F}(Q,t) + \int_0^t dt' M^{(2)}(Q,t-t')\dot{F}(Q,t') + \langle\omega_Q^2\rangle F(Q,t) = 0, \tag{6}$$

where the dots denote time derivatives and different choices of $M^{(2)}(Q,t)$ lead to different lineshapes for $S(Q,\omega)$, i.e., the frequency spectrum of $F(Q,t)$. In Eq. (6) $F(Q,t)$ has the property of being real and even in time, and the corresponding spectrum, obtained through Fourier transformation, is an even function of frequency. The VE model corresponds to a memory function where both viscous and thermal relaxation follow an exponential decay:

$$M^{(2)}_{\rm VE}(Q,t) = \left[\langle\omega_Q^4\rangle/\langle\omega_Q^2\rangle - \gamma(Q)\langle\omega_Q^2\rangle\right]\exp[-t/\tau(Q)] + [\gamma(Q)-1]\langle\omega_Q^2\rangle\exp[-\Gamma_{\rm T}(Q)t], \tag{7}$$

with $\langle\omega_Q^4\rangle$ the fourth frequency moment of the normalized spectrum $S(Q,\omega)/S(Q)$. In Eq. (7) all parameters (that is, the two time constants τ and $1/\Gamma_{\rm T}$, the reduced fourth frequency moment, and γ) are unknown functions of Q except for their $Q \to 0$ behavior given by the predictions of linearized hydrodynamic theory.[7,36,46,56] The GH memory function is simply obtained if the first exponential in Eq. (7) is substituted by an instantaneous relaxation in the form of a δ function:

$$M^{(2)}_{\rm GH}(Q,t) = 2B(Q)\delta(t) + [\gamma(Q)-1]\langle\omega_Q^2\rangle\exp[-\Gamma_{\rm T}(Q)t], \tag{8}$$

where, in the $Q \to 0$ limit, $B(Q)$ has a Q^2 dependence and $\gamma(Q)$ reduces to the specific-heat ratio.[46] In the GH case, solution of Eq. (6) leads to the Rayleigh-Brillouin triplet of Eq. (4), while with the VE memory function it can be shown[46] that a four-line spectrum is obtained, with an additional central

Lorentzian of amplitude a_2 and half width z_2:

$$S_{\rm VE}(Q,\omega) = \frac{S(Q)}{\pi}\left[a_0\frac{z_0}{\omega^2+z_0^2} + a_2\frac{z_2}{\omega^2+z_2^2} + a_{\rm s}\frac{z_{\rm s}+b_{\rm s}(\omega+\omega_{\rm s})}{(\omega+\omega_{\rm s})^2+z_{\rm s}^2} + a_{\rm s}\frac{z_{\rm s}-b_{\rm s}(\omega-\omega_{\rm s})}{(\omega-\omega_{\rm s})^2+z_{\rm s}^2}\right]. \quad (9)$$

In the above equation the dependence on Q of the various parameters has been omitted to shorten the notation. Exact relationships given in Ref. 46 permit the calculation of the corresponding parameters of the memory function of Eq. (7).

The simulated spectra of liquid gold were fitted with both models and an example of the results is shown in Fig. 6 at two Q values. It can be observed that a VE description better accounts for the overall data and for the inelastic peak position, especially at shorter length scales. For this reason we focus on the VE results for the discussion of liquid gold dynamics.

Before doing so, however, we note in Fig. 6 that the GH fit deviates from the simulated $S(Q,\omega)$ in much the same way as does the GH fit to the experimental data (see Fig. 5). This observation supports the statement of a superior modeling provided by the VE lineshape, and suggests that an even better agreement would have been found with the neutron spectra,

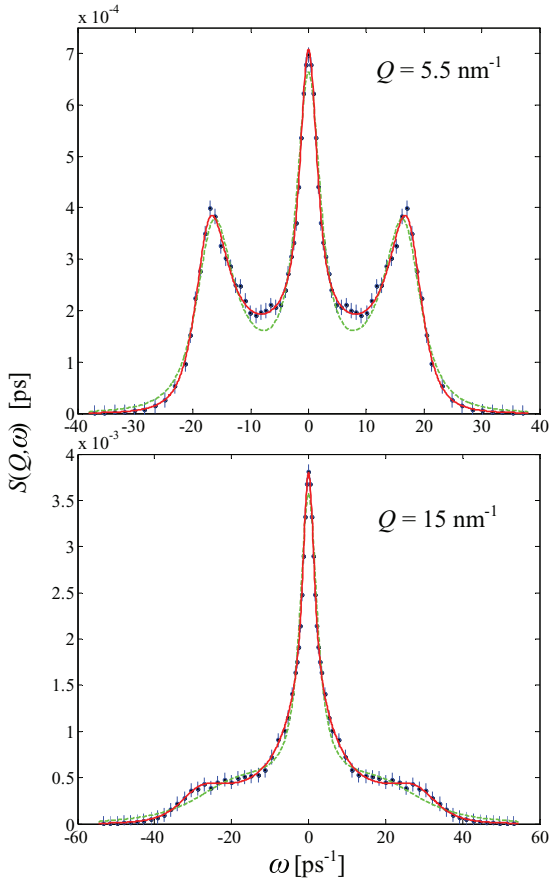

FIG. 6. (Color online) Dynamic structure factor of liquid gold as obtained by means of *ab initio* simulations (dots with error bars) at two example wave vectors. Fit results obtained by a GH (dashed green curve) and a VE (solid red line) modeling of the simulation data are compared.

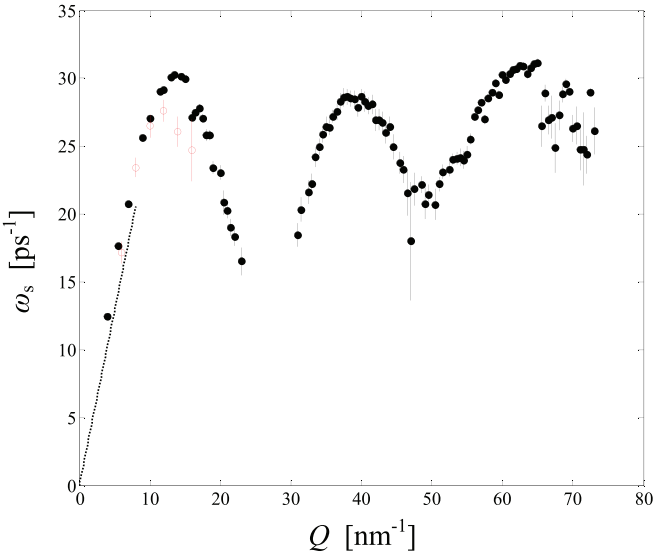

FIG. 7. (Color online) Dispersion curve obtained from the VE fits of the simulated spectra (full circles with error bars). The red circles are the corresponding experimental results already shown in Fig. 4. The straight line is the linearized hydrodynamics prescription. Data are missing around the position of the main maximum in the static structure factor due to the instability of the fit results in such a wave-vector region (see text).

had it been possible to use $S_{\rm VE}(Q,\omega)$ in Eq. (3). As already said, this more-refined analysis was not possible simply because it would have required too large a number of free parameters in a fit function due to account also for multiple-scattering intensity and absolute normalization. On the other hand, when the lineshape fitting is performed on data which represent directly the dynamic structure factor alone, use of $S_{\rm VE}(Q,\omega)$ becomes possible.

Figure 7 shows the dispersion curve of the excitation frequency $\omega_{\rm s}$ of Eq. (9) in the wide Q range explored by simulations. Just for comparison, the experimental GH results of Fig. 4 are also reported. Unfortunately, the available simulation data are presently not accurate enough in the region around Q_p, where typically fits become more demanding because of the transition to overdamped acoustic modes, with loss of oscillatory behavior and vanishing frequency, at the borders of the first pseudo-Brillouin zone of liquids. When this occurs, the lineshape (9) is changed into the sum of four symmetric Lorentzian lines all centered at zero frequency. Anyway, the lack of reliable fit results around 26 nm^{-1} does not prevent us from appreciating the typical behavior of the excitation energy with growing Q, independently of the conducting or insulating nature of the liquid. The other dynamical parameters in gold also display similar trends as those observed in other liquids[7,36] if a viscoelastic analysis is consistently applied to all of them. In particular, in Fig. 8 we show the Q dependence of the characteristic frequency Ω and damping rate $z_{\rm s}$, related to the excitation frequency by the typical damped-oscillator relationship $\omega_{\rm s} = \sqrt{\Omega^2 - z_{\rm s}^2}$. The comparison with Fig. 3(a) of Ref. 7 and Fig. 10(a) of Ref. 36 also provides evidence of the mentioned resemblance in the behavior of the acoustic modes among fluids of different nature.

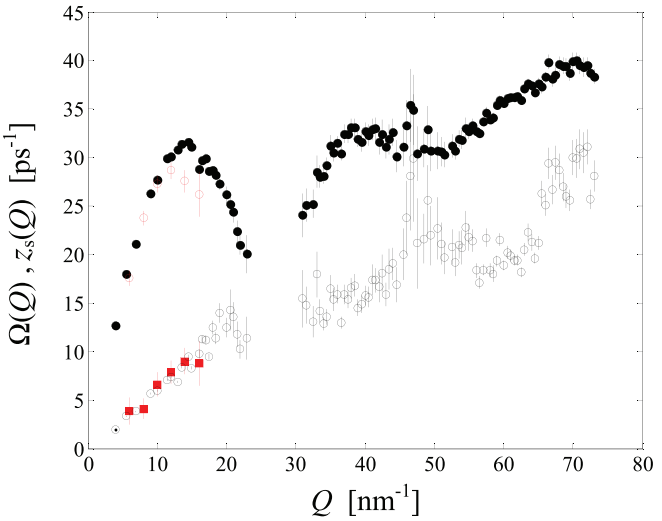

FIG. 8. (Color online) Q dependence of the undamped frequency $\Omega(Q)$ (full circles with error bars) and the damping z_s (black circles with error bars) of the VE equivalent harmonic oscillator representing the collective excitations in liquid gold, obtained from the VE fit to the simulated spectra. The red circles and red squares are the corresponding experimental results already shown for z_s in Fig. 4.

This striking dynamical similarity among disparate liquids is better evidenced by the direct comparison of available dispersion curves for the translational collective modes of systems we analyzed with the same criteria adopted here for gold. For this purpose, Fig. 9 shows a comparison among the excitation frequencies $\omega_s(Q)$ of gold and of two simple molecular liquids such as liquid carbon dioxide[36] and liquid deuteromethane.[7] In addition, a preliminary dispersion curve obtained from a viscoelastic analysis of our *ab initio* simulations of liquid cadmium is also shown.[19] It is clear that, apart from the absolute values of the excitation energies, the translational dynamics of metals and insulators in the liquid phase shows no qualitative differences. Moreover, for the two metals we considered until now, we found no need to resort to more complex models (as sometimes reported for alkali metals[10]) to perfectly describe the Au and Cd spectra, provided parameters are left free to vary with Q and not imposed unphysical constraints, especially with decreasing the length scale.

At this level of comparison, similarities are unexpectedly remarkable but limited to the qualitative behavior of the dynamical parameters. Conversely, a deeper resemblance seems to exist among the dynamic response of different liquids. A quite convincing proof of this strong, nearly system-independent, physical property is given in Fig. 10, where the ratio of the damping to the frequency of the collective sound modes is plotted as a function of Q/Q_p for the four liquids of Fig. 9, after an approximate scaling, for instance, to the CO_2 values. The plotted curves were obtained by multiplying

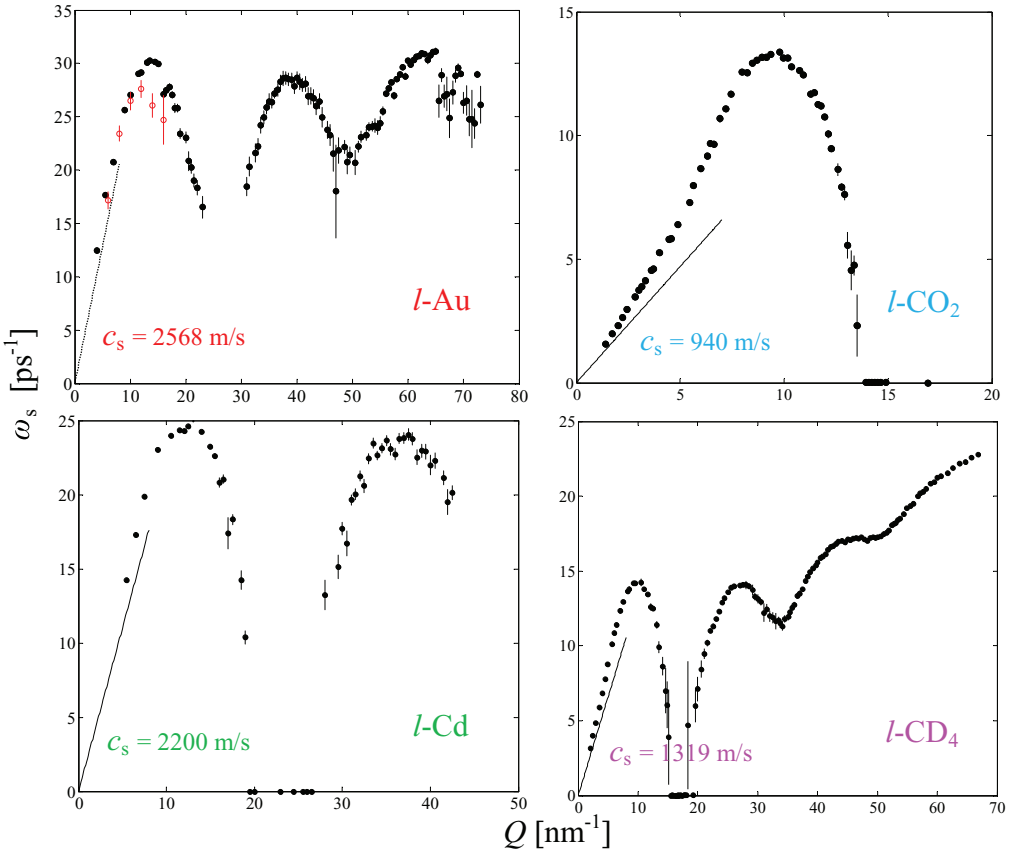

FIG. 9. (Color online) Dispersion curves and their hydrodynamic asymptotes for different liquids as obtained by consistent VE analysis of available simulation data. The center-of-mass dynamics of acoustic excitations in liquid CO_2 and CD_4 is compared to that of liquid Au and Cd. In each frame the liquid under consideration is directly specified. The top-left frame is the same as Fig. 7. The plots regarding CO_2 and CD_4 where taken from Refs. 36 and 7, respectively.

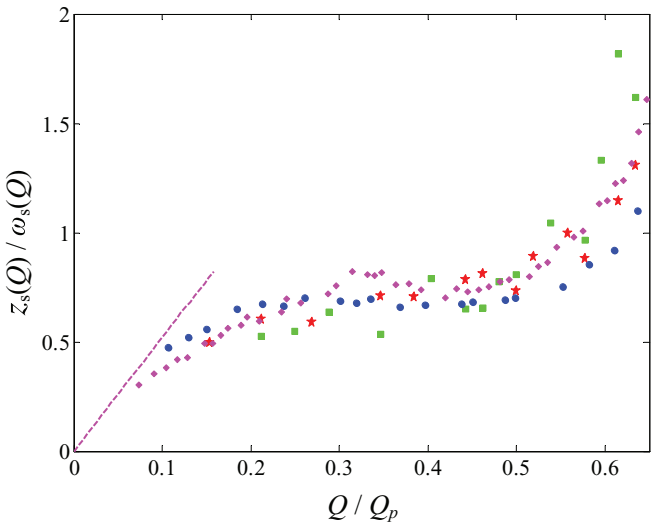

FIG. 10. (Color online) Ratio of damping to frequency of acoustic excitations for the four liquids previously considered. Data for each system have been appositely scaled (see text) to the carbon dioxide values and plotted as a function of Q/Q_p. Note that Cd and Au have the same Q_p value (26 nm^{-1}), just as it happens for CD_4 and CO_2 (19 nm^{-1}). Data for Au (red stars), Cd (green squares), CO_2 (pink diamonds), and CD_4 (blue dots) substantially follow the same curve. The dashed line shows the hydrodynamic behavior of z_s/ω_s for CO_2.

the z_s/ω_s values by 2.00, 3.05, and 3.20 for CD_4, Cd, and Au, respectively. Thus, z_s/ω_s in simple nonmetallic liquids is larger than in liquid metals, but simple scaling factors bring the ratios for the various systems to lie on the same curve in the whole Q range. The variation of such scale factors is mainly related to the spread of the sound velocities among the various fluids.

Two points are worth noting as far as the property displayed in Fig. 10 is concerned. One is that no such scaling works for either z_s or ω_s separately. Moreover, it is an obvious result that z_s/ω_s is linear in Q in the hydrodynamic limit, where $z_s \approx \Gamma Q^2$ and $\omega_s \approx c_s Q$, so that a set of factors bringing the slopes Γ/c_s of the various fluids to coincide would provide a perfect scaling. In Fig. 10 we show the hydrodynamic linear ratio z_s/ω_s for CO_2, but it is essential to realize that the corresponding straight lines of the other liquids coincide with it if multiplied by 1.10, 0.26, and 0.06 for CD_4, Cd, and Au, respectively, i.e., using scaling factors that are completely different from those used in the experimental Q range and grow in reverse order. In other words, within the hydrodynamic regime, z_s/ω_s is *larger* in metals.

This result, far from being an unexplained anomaly, is again a confirmation of the fully nonhydrodynamic nature of the damping parameters of liquid metals in the Q range accessible to spectroscopic techniques at the nanometer scale. In fact, while in the hydrodynamic range it would be the thermal diffusion of metals to play the dominant role, at the explored Q values the damping-to-frequency ratio is reduced, in metallic liquids, by the higher sound speed while the damping takes values comparable to those of nonconducting fluids.

The important result is then that the Q dependence of z_s/ω_s shown in Fig. 10 is a common property of different fluids which is valid well outside the hydrodynamic regime. It is also interesting to note that, if the comparison is limited to the two metals only, there is substantial agreement of the damping-to-frequency ratios even without scaling, i.e., in absolute units, since the scaling factors for Au and Cd are similar (3.20 and 3.05 respectively). Moreover, the wave-vector renormalization via Q_p indicates that the damping-to-frequency ratio is sensitive to the typical nearest-neighbor distances of a dense liquid.

This finding is interesting in liquid-state physics because it indicates that the propagation and damping of sound waves at the nanometer length scale is to a large extent uninfluenced by the presence or absence of an electron sea. The mentioned hypothesis about the reasons why experimental damping rates of liquid metals are dramatically lower than the hydrodynamic ones, which instead depend on properties governed by the conduction electrons, seems therefore to find support in the present observations. These lead us to conclude that the collective nanoscale dynamics of liquid metals has no peculiarities with respect to simple insulating liquids and, more important, it is actually ruled by the ionic component.

Of course, metals and insulators in the liquid state are quite different classes of systems, and the main difference obviously resides in the electronic properties. However, the propagation and decay of sound modes are steered by the screened-ion interactions. The contribution of electrons in determining the forces between particles is also different in the two kinds of liquids but seems to play a secondary role whatever densely packed fluid is studied at a nanoscopic level.

VI. CONCLUSIONS

This work revealed to be quite a rich source of information in several aspects. From the experimental side, technical difficulties related to the high melting temperature of gold were satisfactorily overtaken by a careful choice of the cell material, despite the difficult machining. However, a most important experimental achievement is that the present data on gold provide another convincing proof that neutron measurements on strongly absorbing samples can give unexpectedly good results and opens the use of neutrons to many unexplored systems. The BRISP spectrometer confirms its suitability to efficiently probe collective dynamics in fluids with high sound speed. As far as data analysis, modeling, and simulations are concerned, this neutron study on liquid gold confirmed the crucial importance of multiple-scattering subtraction in inelastic-scattering determinations of the dynamic structure factor, even for weakly scattering systems. Moreover, we found that neutron data are satisfactorily described by a generalized hydrodynamics model and compare well with the *ab initio* simulations. The viscoelastic model is anyway shown to be superior in describing the collective dynamics of liquids in the whole Q range more comfortably probed by simulation methods.

The frequency spectrum of a time-dependent autocorrelation of any dynamical variable has been demonstrated in a recent theoretical work[57] to have the fundamental property of being represented by an infinite sum of Lorentzian lines. In practice, the true theoretical expression of the actual spectrum needs then to be approximated by a suitable truncation, leading

to a sum of a finite number of Lorentzian functions whose parameters assume the meaning of characteristic damping constants and, if nonzero imaginary parts are present, characteristic frequencies of the system. This finite representation is thus perfectly contained in the GH or VE modeling of our spectra, which fully complies with a realistic application of the general result of Ref. 57. Indeed, the various widely used models of the second-order memory function can all be shown to lead to a spectrum composed of a sum of an appropriate number of Lorentzian lines,[46] although this universal property of the lineshape has long remained unnoticed. Going beyond this recognition, our investigation of liquid Au also provides evidence that, among a variety of such possibilities, the choice of the model to be fitted without imposing arbitrary constraints or useless overparametrizations is becoming an important issue in the microscopic physics of fluids.[3]

Valuable scientific knowledge was gifted by this investigation of liquid gold. Indeed, no substantial differences are observed in the overall collective properties when switching from conducting to insulating liquids, except for the much more marked deviation of the damping rates, in metals, from hydrodynamic behavior. Beyond expectations, a nearly universal behavior is suggested for liquids of any nature, scarcely sensitive to the presence of an electron sea at sufficiently small length scales.

ACKNOWLEDGMENTS

We wish to thank the ILL personnel for their precious support during the measurements in Grenoble. We are grateful to Simone Aisa (Dipartimento di Fisica, Università di Perugia, Italy) for his skillful realization of the sample container.

[1] J. R. D. Copley and J. M. Rowe, Phys. Rev. Lett. **32**, 49 (1974).
[2] O. Söderström, J. R. D. Copley, J.-B. Suck, and B. Dorner, J. Phys. F: Met. Phys. **10**, L151 (1980).
[3] W. Montfrooij and I. de Schepper, *Excitations in Simple Liquids, Liquid Metals and Superfluids* (Oxford University Press, New York, 2010).
[4] S. W. Lovesey, Phys. Rev. Lett. **53**, 401 (1984).
[5] S. Blairs, J. Colloid Interface Sci. **302**, 312 (2006).
[6] E. Guarini, U. Bafile, F. Barocchi, F. Demmel, F. Formisano, M. Sampoli, and G. Venturi, Europhys. Lett. **72**, 969 (2005).
[7] M. Sampoli, U. Bafile, F. Barocchi, E. Guarini, and G. Venturi, J. Phys.: Condens. Matter **20**, 104206 (2008).
[8] U. Dahlborg, W. Gudowski, and M. Davidovic, J. Phys.: Condens. Matter **1**, 6173 (1989).
[9] O. Söderström, Phys. Rev. A **23**, 785 (1981).
[10] T. Scopigno, U. Balucani, G. Ruocco, and F. Sette, J. Phys.: Condens. Matter **12**, 8009 (2000); Phys. Rev. E **65**, 031205 (2002).
[11] L. E. Bove, B. Dorner, C. Petrillo, F. Sacchetti, and J.-B. Suck, Phys. Rev. B **68**, 024208 (2003); T. Bodensteiner, Chr. Morkel, W. Gläser, and B. Dorner, Phys. Rev. A **45**, 5709 (1992); P. H. K. de Jong, P. Verkerk, and L. A. de Graaf, J. Phys.: Condens. Matter **6**, 8391 (1994); A. G. Novikov, V. V. Savostin, A. L. Shimkevich, and M. V. Zaezjev, Phys. B (Amsterdam, Neth.) **234-236**, 359 (1997); H. Sinn, F. Sette, U. Bergmann, Ch. Halcoussis, M. Krisch, R. Verbeni, and E. Burkel, Phys. Rev. Lett. **78**, 1715 (1997); A. Monaco, T. Scopigno, P. Benassi, A. Giugni, G. Monaco, M. Nardone, G. Ruocco, and M. Sampoli, J. Chem. Phys. **120**, 8089 (2004); M. D. Ruiz-Martín, M. Jiménez-Ruiz, A. Stunault, F. J. Bermejo, R. Fernández-Perea, and C. Cabrillo, Phys. Rev. B **76**, 174201 (2007).
[12] L. E. Bove, F. Sacchetti, C. Petrillo, B. Dorner, F. Formisano, and F. Barocchi, Phys. Rev. Lett. **87**, 215504 (2001).
[13] L. E. Bove, F. Sacchetti, C. Petrillo, B. Dorner, F. Formisano, M. Sampoli, and F. Barocchi, Phil. Mag. B **82**, 365 (2002).
[14] S. Hosokawa, H. Sinn, F. Hensel, A. Alatas, E. E. Alp, and W.-C. Pilgrim, J. Non-Cryst. Solids **312-314**, 163 (2002).
[15] L. E. Bove, F. Formisano, F. Sacchetti, C. Petrillo, A. Ivanov, B. Dorner, and F. Barocchi, Phys. Rev. B **71**, 014207 (2005); F. J. Bermejo, R. Fernández-Perea, M. Alvarez, B. Roessli, H. E. Fischer, and J. Bossy, Phys. Rev. E **56**, 3358 (1997); V. M. Giordano and G. Monaco, Phys. Rev. B **84**, 052201 (2011); S. Hosokawa *et al*., Phys. Rev. Lett. **102**, 105502 (2009); M. Patty, K. Schoen, W. Montfrooij, and Z. Yamani, J. Non-Cryst. Solids **357**, 1000 (2011); T. Scopigno, A. Filipponi, M. Krisch, G. Monaco, G. Ruocco, and F. Sette, Phys. Rev. Lett. **89**, 255506 (2002).
[16] S. Cazzato, T. Scopigno, S. Hosokawa, M. Inui, W.-C. Pilgrim, and G. Ruocco, J. Chem. Phys. **128**, 234502 (2008).
[17] M. D. Ruiz-Martín, M. Jiménez-Ruiz, M. Plazanet, F. J. Bermejo, R. Fernández-Perea, and C. Cabrillo, Phys. Rev. B **75**, 224202 (2007).
[18] F. Sacchetti *et al*. (unpublished).
[19] F. Formisano *et al*. (unpublished).
[20] T. Scopigno, U. Balucani, G. Ruocco, and F. Sette, Phys. Rev. E **63**, 011210 (2000).
[21] U. Dahlborg and L. G. Olsson, J. Phys. F: Met. Phys. **13**, 555 (1983); L. Sani, L. E. Bove, C. Petrillo, and F. Sacchetti, J. Non-Cryst. Solids **353**, 3139 (2007).
[22] S. Hosokawa, J. Greif, F. Demmel, and W.-C. Pilgrim, Chem. Phys. **292**, 253 (2003).
[23] S. Hosokawa, M. Inui, K. Matsuda, D. Ishikawa, and A. Q. R. Baron, Phys. Rev. B **77**, 174203 (2008).
[24] Y. Kawakita *et al*., J. Phys. Soc. Jpn. **72**, 1603 (2003).
[25] A. H. Said, H. Sinn, A. Alatas, C. A. Burns, D. L. Price, M. L. Saboungi, and W. Schirmacher, Phys. Rev. B **74**, 172202 (2006).
[26] S. Hosokawa, W.-C. Pilgrim, Y. Kawakita, S. Takeda, A. Q. R. Baron, D. Ishikawa, and S. Tsutsui, J. Non-Cryst. Solids **353**, 3149 (2007); F. Sacchetti, P. Bosi, and F. Menzinger, J. Phys. C **15**, 4483 (1982); M. Inui, S. Hosokawa, K. Matsuda, S. Tsutsui, and A. Q. R. Baron, Phys. Rev. B **77**, 224201 (2008); S. Hosokawa, W.-C. Pilgrim, F. Demmel, and F. Albergamo, J. Non-Cryst. Solids **352**, 5114 (2006); Y. Kajihara, M. Inui, S. Hosokawa, K. Matsuda, and A. Q. R. Baron, J. Phys.: Condens. Matter **20**, 494244 (2008); M. D. Ruiz-Martín, M. Jiménez-Ruiz, F. J. Bermejo, and R. Fernández-Perea, Phys. Rev. B **73**, 094201 (2006).
[27] L. E. Bove, F. Sacchetti, C. Petrillo, and B. Dorner, Phys. Rev. Lett. **85**, 5352 (2000).
[28] S. Jahn and J.-B. Suck, Phys. Rev. Lett. **92**, 185507 (2004).

[29]L. E. Bove, F. Formisano, E. Guarini, A. Ivanov, C. Petrillo, and F. Sacchetti, Europhys. Lett. **79**, 16002 (2007).
[30]C. A. Burns, P. Abbamonte, E. D. Isaacs, and P. M. Platzman, Phys. Rev. Lett. **83**, 2390 (1999).
[31]C. A. Burns, P. M. Platzman, H. Sinn, A. Alatas, and E. E. Alp, Phys. Rev. Lett. **86**, 2357 (2001).
[32]F. Sacchetti, E. Guarini, C. Petrillo, L. E. Bove, B. Dorner, F. Demmel, and F. Barocchi, Phys. Rev. B **67**, 014207 (2003).
[33]C. Petrillo, F. Sacchetti, E. Guarini, L. E. Bove, and F. Demmel, Phys. Rev. B **84**, 094206 (2011).
[34]E. Guarini, M. Sampoli, G. Venturi, U. Bafile, and F. Barocchi, Phys. Rev. Lett. **99**, 167801 (2007).
[35]E. Guarini, M. Sampoli, U. Bafile, F. Formisano, M. Jiménez-Ruiz, A. Orecchini, G. Venturi, and F. Barocchi, Chem. Phys. Lett. **464**, 177 (2008).
[36]M. Sampoli, U. Bafile, E. Guarini, and F. Barocchi, Phys. Rev. B **79**, 214203 (2009).
[37]G. M. Bhuiyan, L. E. González, and D. J. González, Condens. Matter Phys. **15**, 33604 (2012).
[38]Y. Waseda and M. Ohtani, Phys. Status Solidi B **62**, 535 (1974).
[39]L. J. Norrby, J. Chem. Edu. **68**, 110 (1991).
[40]L. J. Munro, J. K. Johnson, and K. D. Jordan, J. Chem. Phys. **114**, 5545 (2001).
[41]C. F. Kunz, C. Hättig, and B. A. Hess, Mol. Phys. **89**, 139 (1996).
[42]D. Aisa *et al.*, Nucl. Instrum. Methods Phys. Res., Sect. A **544**, 620 (2005).
[43]*CRC Handbook of Chemistry and Physics*, 59th ed. (Robert C. Weast, West Palm Beach, 1979).
[44]A. Bogicevic, L. B. Hansen, and B. I. Lundqvist, Phys. Rev. E **55**, 5535 (1997).
[45]A. De Francesco, U. Bafile, F. Formisano, and E. Guarini, J. Phys.: Conf. Ser. **340**, 012024 (2012).
[46]U. Bafile, E. Guarini, and F. Barocchi, Phys. Rev. E **73**, 061203 (2006).
[47]N. H. March, *Liquid Metals* (Cambridge University Press, Cambridge, 1990).
[48]T. E. Faber, *An Introduction to the Theory of Liquid Metals* (Cambridge University Press, Cambridge, 1972).
[49]C. Y. Ho, R. W. Powell, and P. E. Liley, J. Phys. Chem. Ref. Data **1**, 279 (1972).
[50]G. Kresse and J. Hafner, Phys. Rev. B **47**, 558 (1993).
[51]W. Kohn and L. Sham, Phys. Rev. **140**, A1133 (1965).
[52]J. P. Perdew, K. Burke, and M. Ernzerhof, Phys. Rev. Lett. **77**, 3865 (1996).
[53]P. E. Blöchl, Phys. Rev. B **50**, 17953 (1994).
[54]G. Kresse and D. Joubert, Phys. Rev. B **59**, 1758 (1999).
[55]T. Rog, K. Murzyn, K. Hinsen, and G. R. Kneller, J. Comput. Chem. **24**, 657 (2003).
[56]U. Balucani and M. Zoppi, *Dynamics of the Liquid State* (Clarendon, Oxford, 1994).
[57]F. Barocchi, U. Bafile, and M. Sampoli, Phys. Rev. E **85**, 022102 (2012).